ACS POLYMERS Au
AN OPEN ACCESS JOURNAL OF THE AMERICAN CHEMICAL SOCIETY

pubs.acs.org/polymerau
Letter

Observing Depolymerization of a RAFT Polymer by Time-Resolved Small-Angle X ray Scattering

Rintaro Takahashi* and Ayae Sugawara-Narutaki

Cite This: ACS Polym. Au 2025, 5, 129−133

ABSTRACT: Recently, it has been reported that various polymethacrylates synthesized via reversible addition−fragmentation chain-transfer (RAFT) polymerization may be depolymerized by heating them to 120 °C in solution. However, insights into the mechanisms and kinetics remain limited. In this work, we monitored the depolymerization process of poly(benzyl methacrylate) in *p*-xylene using time-resolved small-angle X-ray scattering (SAXS). The results revealed that the weight-average molecular weight gradually decreased, while the z-average radius of gyration remained almost unchanged until approximately half of the repeating units were converted. This unexpected behavior could be well-reproduced by a kinetic model of end-to-end depolymerization (unzipping). This study provides the first direct observation of the structural evolution during depolymerization via an unzipping mechanism.

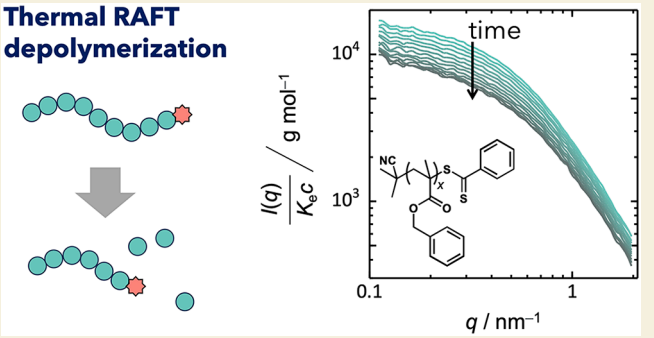

KEYWORDS: *Depolymerization, Time-resolved small-angle X-ray scattering, Unzipping, Reversible addition−fragmentation chain-transfer polymerization, Kinetics*

Plastics are integral to our daily lives and the global economy due to their durability, lightweight nature, and cost-effectiveness. However, micro- and nanoplastics pose a significant threat to marine ecosystems.[1−3] Within the scientific community, numerous studies have focused on polymerization and the creation of durable and functional plastics, whereas much fewer studies have been conducted on depolymerization and upcycling.[1,4−6] One of the major advancements in the field of polymerization is the reversible-deactivation radical polymerization, including reversible addition−fragmentation chain-transfer (RAFT) polymerization and atom-transfer radical polymerization (ATRP). These techniques allow for precise control over the molecular weight, composition, and architecture of polymers, leading to materials with tailored properties for specific applications. RAFT polymerization, in particular, is applicable to a wide range of monomer types without the necessity of metals and is now essential for creating advanced materials in fields such as optoelectronics, adhesives, hydraulic fluids, membranes, biosensors, and drug delivery.[7−13]

On the other hand, the realization of controlled depolymerization remains a challenging topic, which will contribute to the long-term sustainability of our society. Recently, the group of Anastasaki[5,14−18] discovered that various polymethacrylates synthesized through RAFT polymerization could be depolymerized simply by heating them to 120 °C in dilute solution, without the need for any catalyst. Notably, a maximum conversion of 92% was achieved, although this high conversion was observed only at a dilute monomer unit concentration of 5 mM. Additionally, a polymethacrylate-based hydrogel prepared via RAFT polymerization exhibited a gel-to-sol transition upon depolymerization. This method therefore holds potential for the upcycling of methacrylate-based plastics. However, mechanistic and kinetic understanding remains limited, and the *absolute* molecular weight has not been obtained; studies to date have relied on techniques such as ^{1}H nuclear magnetic resonance (NMR), ultraviolet (UV) and mass spectroscopies, and size-exclusion chromatography (SEC).[14−18]

In this study, time-resolved small-angle X-ray scattering (SAXS) was used to monitor the depolymerization process. Small-angle scattering directly measures *absolute* molecular weight and provides *in situ* structural information, such as conformation of polymer chains.[19−21] Although small-angle scattering offers a unique advantage, it has rarely been employed to study depolymerization, as these reactions typically occur at temperatures exceeding the capability of apparatus and sample cells. In this letter, we aim not only to provide insights into the kinetics and mechanisms of

Received: December 4, 2024
Revised: February 10, 2025
Accepted: February 11, 2025
Published: February 13, 2025

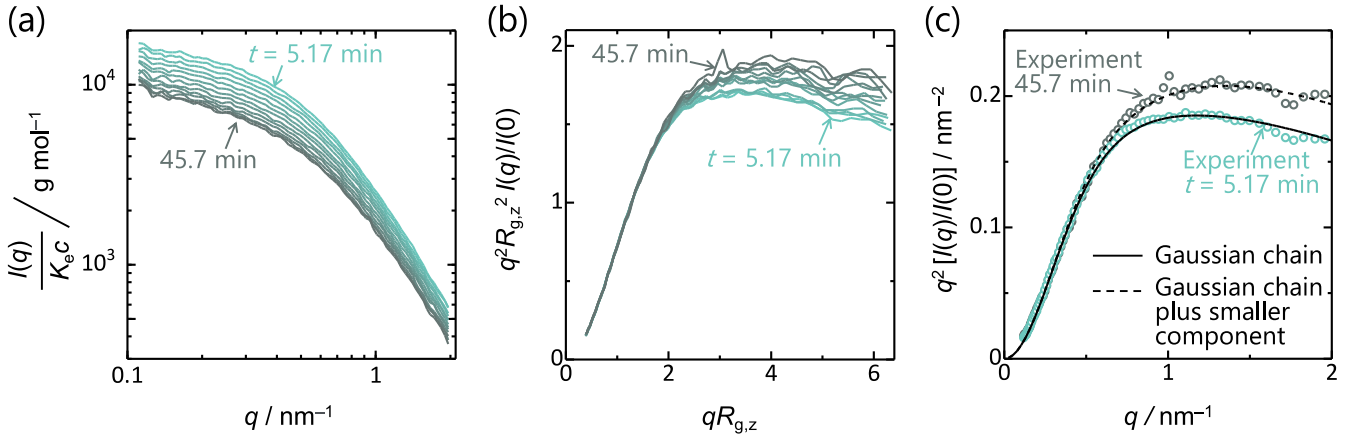

Figure 1. (a) Time evolution of the SAXS profile during the depolymerization of PBzMA bearing a RAFT end-group in *p*-xylene (c = 0.1 wt %) at 120 °C as the double-logarithmic plot. The color corresponds to the time point; the time elapses from the turquoise curve (5.17 min; the first frame) to the gray curve (45.7 min). (b) The same data represented as the dimensionless Kratky plot. (c) Comparison between the model scattering functions (solid and broken black curves; eqs S6 and S7) and the experimentally obtained data at t = 5.17 and 45.7 min (unfilled circles) in the Kratky plot.

depolymerization of a RAFT polymer bearing a RAFT end-group but also to demonstrate the usefulness of small-angle scattering in investigating depolymerization.

As the test sample, we selected poly(benzyl methacrylate) (PBzMA), prepared via RAFT polymerization using 2-cyano-2-propyl benzodithioate (CTA), as this CTA has been reported to exhibit high depolymerization conversion.[14] The synthesized PBzMA had a weight-average molecular weight (M_w) of 17,200, a weight-average degree of polymerization (x_w) of 97.7, and a dispersity of the molecular weight ($Đ$) of 1.12. Although lower molecular weight is known to result in higher depolymerization conversion,[15] higher molecular weight is advantageous for scattering experiments due to its correlation with scattering intensity. This molecular weight was therefore chosen in this study. Detailed molecular characteristics of the PBzMA sample are provided in the Supporting Information. For the solvent during depolymerization, *p*-xylene was chosen due to its suitably high boiling point (138 °C), which allows for SAXS measurements using a thin-walled (0.01 mm) capillary cell at the depolymerization temperature of 120 °C. Thinner cell walls lead to better data quality but offer less pressure resistance. Among solvents with sufficiently high boiling points, xylene was deemed optimal for achieving higher depolymerization conversion.[15] For a similar reason, BzMA, with its high boiling point, was chosen over methyl methacrylate, as the type of methacrylate monomer is not expected to significantly influence depolymerization conversion.[14] On the basis of previous reports,[14,15] this system (PBzMA in xylene, with x_w of 97.7) is expected to achieve a depolymerization conversion of approximately 50 mol % in monomer unit. Under these conditions, each polymer chain is expected to depolymerize individually like the reverse process of free radical polymerization, rather than having most chains depolymerize simultaneously.[17]

For the SAXS measurements, the PBzMA/*p*-xylene solution was deoxygenated by nitrogen sparging. The polymer concentration (c) was 0.1 or 0.2 wt %, corresponding to 5 or 10 mM in the monomer unit, respectively, as it was reported that higher concentrations exhibit lower conversion in the depolymerization (see Figure S4 in ref 13), as the appearance of the monomer influences the polymer−monomer equilibrium. The solution was heated to 120 °C, followed by time-resolved SAXS measurements under a nitrogen atmosphere to capture the time evolution of the SAXS profiles. On the vertical axis of the obtained SAXS profiles (Figure 1a), $I(q)$ represents the differential scattering cross-section as a function of the length of the scattering vector (q). It is divided by the optical constant in X-ray scattering (K_e)[21,22] and c, resulting in a unit of g/mol. The SAXS profile clearly exhibits a monotonical decrease in $I(q)/K_ec$ over time, evidencing the decrease in the molecular weight of PBzMA, as $I(q)$ generally follows $\lim_{q\to 0, c\to 0} I(q) = M_w c K_e$, which is derived without assuming any specific model.[21] Meanwhile, the slope in the low-q region appears to remain unchanged, suggesting that the molecular dimensions did not significantly change.

To assess the effect of X-ray exposure, a control experiment was conducted using a PBzMA/*p*-xylene solution without deoxygenation (*i.e.*, without nitrogen sparging). The solution was heated to 120 °C, and time-resolved SAXS measurements were performed. The absence of depolymerization under this condition was confirmed by ^{1}H NMR (Figures S5 and S6). Consequently, the SAXS profiles remained unchanged (Figure S7), confirming that exposures of the high-flux X-ray did not cleave the polymer chains. This result also demonstrates that the X-ray exposure did not promote depolymerization, despite the general properties of X-rays to generate radicals and often promote radical polymerization.[23] Furthermore, the fidelity of CTA remained, and the chain end did not undergo thermolysis under this thermal condition (120 °C for 1 h) (Figure S5), although polymethacrylates are known to undergo thermolysis, yielding vinyl end groups, under more intense conditions (heating to 60 °C for 30 h[24] or heating at a rate of 5 °C/min to 240 °C[25]).

We analyzed the SAXS profiles in the initial and final states as dimensionless Kratky plots (Figure 1b), constructed with the form factor $[I(q)/I(0)]$ as well as the z-average radius of gyration ($R_{g,z}$) derived from the Berry plots explained later. The Kratky plot highlights local structures more than the double-logarithmic plots of $I(q)$ and q do. Remarkably, the high-q scattering in the Kratky plot increases over time; this behavior was analyzed by a model scattering function. As a result, the Gaussian chain model with R_g = 3 ± 0.05 nm, considering the cross-sectional diameter of 1 ± 0.1 nm (eq

https://doi.org/10.1021/acspolymersau.4c00095
ACS Polym. Au 2025, 5, 129−133

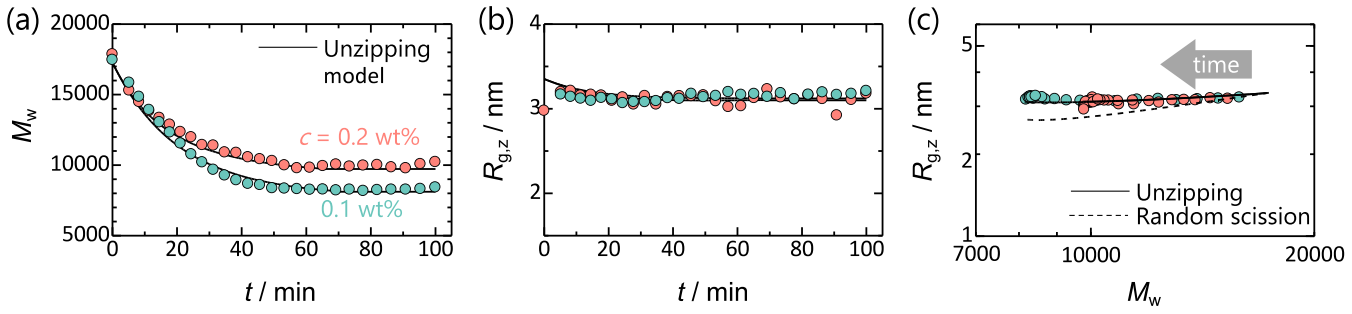

Figure 2. Time evolution of M_w (a) and $R_{g,z}$ (b), as well as the double-logarithmic plot of $R_{g,z}$ against M_w (c) for c = 0.1 wt % (turquoise symbol) and 0.2 wt % (pink symbol), derived from the Berry plot (Figure S8). Solid and broken black curves represent the fitted curves of unzipping and random scission models, respectively. The left-most points in Panels a and b were obtained at 25 °C, and these data are not included in Panel c.

S6), nicely fitted the SAXS profiles in the initial state, represented by the solid black curve (Figure 1c). The scattering structure factor or intermolecular interference effect was negligible as the measurements were performed in sufficiently dilute conditions, and we observed no significant difference in the $I(q)/K_ec$ values between c = 0.1 and 0.2 wt %.

At t = 45.7 min, the Gaussian chain model with the same dimensions as in t = 5.17 min failed to fit the high-q region (Figure 1c). This increasing upward deviation in the high-q region over time indicates the emergence of smaller molecules (*i.e.*, the polymers with lower molecular weights, the monomers, and CTA-derived products[16]) via depolymerization. Consequently, we employed a coexistence model consisting of the Gaussian chain with the original dimensions and a smaller Gaussian chain (eq S7). The radius of gyration for the smaller Gaussian chain was 1.2 ± 0.5 nm, and the cross-sectional diameter was assumed to be 1 nm. This coexistence model provided a good fit to the experimental data (broken black curve in Figure 1c). However, the exact values of the radius of gyration and cross-sectional diameter could not be independently determined, and the smaller component could not be analyzed in depth, as it is generally complicated to analyze small quantities of smaller particles precisely in the presence of larger particles by SAXS. Nevertheless, the Kratky plots clearly demonstrate the increasing appearance of the smaller components over time by depolymerization.

Instead of further analysis in terms of the form factor, we analyzed the weight-average molecular weight (M_w) and $R_{g,z}$ as a function of time (t) (Figure 2a and 2b), which were obtained from Berry's root plot[26] (Figure S8 and eq S1). Please note that M_w and $R_{g,z}$ are the averaged values over the polymer and monomer. Intriguingly, M_w decreased over time while $R_{g,z}$ remained constant, which puzzled us when we first saw these data. However, upon considering the kinetic models of depolymerization, we found that this behavior of constant $R_{g,z}$ with decreasing M_w is related to the depolymerization kinetics as explained in the next paragraphs. The small jump in $R_{g,z}$ from 0 to 5.17 min (Figure 2b) was caused by the heating from 25 to 120 °C (the dimension was increased by the thermal fluctuation).

If this depolymerization follows a so-called unzipping process (*i.e.*, sequential scission from one end), the kinetics may be written as[27]

$$\mathrm{P}_{x+1} \underset{k_\mathrm{p}}{\overset{k_\mathrm{d}}{\rightleftharpoons}} \mathrm{P}_x + \mathrm{P}_1 \tag{1}$$

$$\mathrm{P}_x \underset{k_\mathrm{p}}{\overset{k_\mathrm{d}}{\rightleftharpoons}} \mathrm{P}_{x-1} + \mathrm{P}_1 \tag{2}$$

where P_x stands for the x-mer (living chain), and k_d and k_p are the rate constants of depolymerization and polymerization, respectively. During the depolymerization process, the fidelity of CTA lapses. The terminal reaction is reported to be governed by the reactions with the solvent,[16] which are supposed to occur regardless of x, with a rate constant ($\tilde{k}$) as follows:

$$\mathrm{P}_x \xrightarrow{\tilde{k}} \tilde{\mathrm{P}}_x \tag{3}$$

where $\tilde{\mathrm{P}}_x$ signifies the dead chain of the x-mer; *i.e.*, the degree of polymerization of $\tilde{\mathrm{P}}_x$ no longer changes. Indeed, NMR spectra indicate that signals from CTA-derived compounds gradually appeared as depolymerization progressed (Figure S6). In this model, the equilibration of propagating and depropagating radicals is incorporated into the overall framework (eqs 1−3), as time-resolved SAXS cannot detect such specific processes. The kinetic equations are thus given by

$$\frac{\mathrm{d}C_x}{\mathrm{d}t} = k_\mathrm{d}(C_{x-1} - C_x) - k_\mathrm{p}(C_x - C_{x-1})C_1 - \tilde{k}C_x \quad (x \geq 3) \tag{4}$$

$$\frac{\mathrm{d}C_2}{\mathrm{d}t} = k_\mathrm{d}(C_3 - C_2) - k_\mathrm{p}C_2C_1 - \tilde{k}C_2 \tag{5}$$

$$\frac{\mathrm{d}\tilde{C}_x}{\mathrm{d}t} = \tilde{k}C_x \tag{6}$$

where C_x and $\tilde{C}_x$ denote the molar concentrations of P_x and $\tilde{\mathrm{P}}_x$, respectively, and x is restricted to be integer values. The monomer concentration (C_1) is related to the polymer concentration as $C_1(t) = \sum_{x=1}^{\infty} xC_x(0) - \sum_{x=2}^{\infty} x[C_x(t) + \tilde{C}_x(t)]$. Numerical calculations with these equations provide the time dependence of each x-mer fraction (Figure 3). For these calculations, we assumed that the initial state obeys a log-normal distribution[28] with $Đ$ of 1.12, as the molecular weight distribution obtained by SEC approximately matched the log-normal distribution (Figure S2).

With $C_x(t)$ and $\tilde{C}_x(t)$, the time-evolution of x_w and M_w are obtained by

$$\frac{M_w(t)}{M_1} = x_w(t) = \frac{\sum_{x=1}^{\infty} x^2[C_x(t) + \tilde{C}_x(t)]}{\sum_{x=1}^{\infty} x[C_x(t) + \tilde{C}_x(t)]} \tag{7}$$

https://doi.org/10.1021/acspolymersau.4c00095
ACS Polym. Au 2025, 5, 129−133

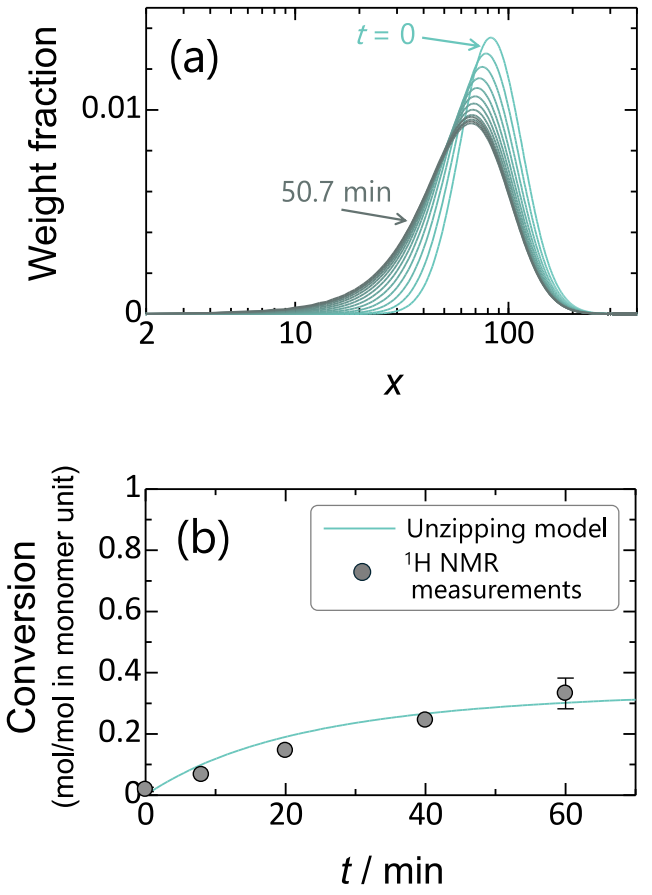

Figure 3. Calculated results of the unzipping model at c = 0.2 wt % as the distribution function of x, including the living and dead chains (a), and the monomer conversion as a function of time (b). The ^{1}H NMR results are also plotted in Panel b (see also Figure S6 for the ^{1}H NMR spectra).

where M_1 stands for the molecular weight of the monomer. In addition, the z-average mean-square radius of gyration can also be calculated as a function of time as follows:

$$R_{g,z}^2(t) = \frac{\sum_{x=1}^{\infty} x^2[C_x(t) + \tilde{C}_x(t)]R_{g,z}^2}{\sum_{x=1}^{\infty} x^2[C_x(t) + \tilde{C}_x(t)]} \quad (8)$$

Here, the radius of gyration of the x-mer ($R_{g,x}$) was calculated by $R_{g,x} = R_{g,1}x^{\nu}$, where $R_{g,1}$ was treated as an adjustable parameter and individually determined to be 0.32 nm by the relationship between $R_{g,z}$ and x. Flory exponent (ν) was set to 0.5 based on the SAXS profiles, which exhibited $I(q) \sim q^{1/\nu} = q^{2.0}$ in the high q region.[29]

In this kinetic model, there are three parameters: k_d, k_p, and $\tilde{k}$. The values of these parameters were determined through fitting as follows. Initially, $M_w(t)$ was fitted by iteratively adjusting these values, with the restriction that the same k_d, k_p, and $\tilde{k}$ can reproduce both experiments with c = 0.1 and 0.2 wt %. Consequently, we found that the $M_w(t)$ values for both concentrations were fitted with k_d = 1.32 ± 0.03 min^{-1}, k_p = 0.32 ± 0.03 min^{-1} mM^{-1}, and $\tilde{k}$ = 0.02 ± 0.002 min^{-1}. Notably, these k_d, k_p, and $\tilde{k}$ values nicely reproduced the constant $R_{g,z}(t)$ behavior. The fitted curves are represented by the solid black curves in Figures 2a and 2b. Furthermore, this model also replicated the conversion obtained by ^{1}H NMR spectroscopy (Figure 3b), thereby supporting the validity of the kinetic model.

Whereas, if the depolymerization mechanism is governed by random scission (the equations are given in the Supporting Information), the constant $R_{g,z}(t)$ behavior cannot be replicated. This is clearly seen in the plot of $R_{g,z}(t)$ against $M_w(t)$ (Figure 2c). The solid curves (unzipping) reproduce the experimentally obtained data, particularly where $R_{g,z}$ remained unchanged while M_w decreased over time. Meanwhile, the broken curve (random scission) fails to replicate this behavior. In the random scission mechanism, the polymer chains rapidly shorten, as any point along the chain may be severed (Figure S4). In contrast, during the unzipping mechanism, the polymer chains remained long for the conversion values (Figure 3a) compared to random scission. $R_{g,z}$ is the z-averaged value, reflecting longer polymer chains rather than shorter ones, whereas M_w is the weight-averaged value. Therefore, the observation of the constant $R_{g,z}$ value holding constant while the M_w value decreases during the depolymerization is indicative of the unzipping mechanism.

In conclusion, the depolymerization of a PBzMA with a RAFT end-group was directly observed *in situ* using time-resolved SAXS measurements. The absolute molecular weight obviously decreased over time, while $R_{g,z}$ remained nearly constant. This behavior stems from the unzipping depolymerization mechanism as well as the z-averaged nature of $R_{g,z}$, as revealed by analysis with the kinetic model of unzipping. To put it another way, this analytical method is useful for obtaining compelling evidence to determine whether the depolymerization follows an unzipping or random scission mechanism, and this study underscores the significance of small-angle scattering when investigating depolymerizations.

■ ASSOCIATED CONTENT

Supporting Information

The Supporting Information is available free of charge at https://pubs.acs.org/doi/10.1021/acspolymersau.4c00095.

Materials and methods; Molecular characteristics of PBzMA (initial state), including ^{1}H NMR spectrum, SEC trace, and SAXS data at 25 °C; Models of the scattering form factor; Kinetic model of the random scission; Time-evolution of the ^{1}H NMR spectrum; SAXS profiles for the nondeoxygenated PBzMA/*p*-xylene solution; Berry plots (PDF)

■ AUTHOR INFORMATION

Corresponding Author

Rintaro Takahashi − *Department of Macromolecular Science, Osaka University, Toyonaka, Osaka 560-0043, Japan;* orcid.org/0000-0003-2168-9436; Email: takahashi@chem.sci.osaka-u.ac.jp

Author

Ayae Sugawara-Narutaki − *Laboratory for Biomaterials and Bioengineering, Institute of Integrated Research, Institute of Science Tokyo, Chiyoda-ku, Tokyo 101-0062, Japan; Department of Energy Engineering, Graduate School of Engineering, Nagoya University, Nagoya, Aichi 464-8603, Japan;* orcid.org/0000-0003-3579-6689

Complete contact information is available at: https://pubs.acs.org/10.1021/acspolymersau.4c00095

https://doi.org/10.1021/acspolymersau.4c00095
ACS Polym. Au 2025, 5, 129−133

Notes

The authors declare no competing financial interest.

■ ACKNOWLEDGMENTS

Japan Synchrotron Radiation Research Institute (JASRI) is acknowledged for the provision of the beam time in SPring-8 (Proposal No. 2023B1174 and 2024A1165). R.T. is grateful to Noboru Ohta (JASRI) for his assistance with the SAXS measurements and Hina Sugimura (Osaka University) for her help during a portion of the NMR measurements. This work was financially supported in part by UBE foundation and JSPS KAKENHI (Grant No. 24K17722).

■ REFERENCES

(1) Korley, L. T. J.; Epps, T. H.; Helms, B. A.; Ryan, A. J. Toward polymer upcycling—adding value and tackling circularity. *Science* **2021**, *373*, 66−69.
(2) MacLeod, M.; Arp, H. P. H.; Tekman, M. B.; Jahnke, A. The global threat from plastic pollution. *Science* **2021**, *373*, 61−65.
(3) Walker, T. R.; Fequet, L. Current trends of unsustainable plastic production and micro(nano) pollution. *Trends Anal. Chem.* **2023**, *160*, No. 116984.
(4) Wang, W.; Alexander, C. Self-Immolative Polymers. *Angew. Chem., Int. Ed.* **2008**, *47*, 7804−7806.
(5) Jones, G. R.; Wang, H. S.; Parkatzidis, K.; Whitfield, R.; Truong, N. P.; Anastasaki, A. Reversed Controlled Polymerization (RCP): Depolymerization from Well-Defined Polymers to Monomers. *J. Am. Chem. Soc.* **2023**, *145*, 9898−9915.
(6) Deng, Z.; Gillies, E. R. Emerging Trends in the Chemistry of End-to-End Depolymerization. *JACS Au* **2023**, *3*, 2436−2450.
(7) Chiefari, J.; Chong, Y. K.; Ercole, F.; Krstina, J.; Jeffery, J.; Le, T. P.; Mayadunne, R. T. A.; Meijs, G. F.; Moad, C. L.; Moad, G.; Rizzardo, E.; Thang, S. H. Living Free-Radical Polymerization by Reversible Addition−Fragmentation Chain Transfer: The RAFT Process. *Macromolecules* **1998**, *31*, 5559−5562.
(8) Hill, M. R.; Carmean, R. N.; Sumerlin, B. S. Expanding the Scope of RAFT Polymerization: Recent Advances and New Horizons. *Macromolecules* **2015**, *48*, 5459−5469.
(9) Perrier, S. 50th Anniversary Perspective: RAFT Polymerization—A User Guide. *Macromolecules* **2017**, *50*, 7433−7447.
(10) Truong, N. P.; Jones, G. R.; Bradford, K. G.; Konkolewicz, D.; Anastasaki, A. A coparison of RAFT and ATRP methods for controlled radical polymerization. *Nat. Rev. Chem.* **2021**, *5*, 859−869.
(11) Peng, W.; Cai, Y.; Fanslau, L.; Vana, P. Nanoengineering with RAFT polymers: from nanocomposite design to applications. *Polym. Chem.* **2021**, *12*, 6198−6229.
(12) Wan, J.; Fan, B.; Thang, S. H. RAFT-mediated polymerization-induced self-assembly (RAFT-PISA): current status and future directions. *Chem. Sci.* **2022**, *13*, 4192−4224.
(13) Destarac, M. Industrial development of reversible-deactivation radical polymerization: is the induction period over? *Polym. Chem.* **2018**, *9*, 4947−4967.
(14) Wang, H. S.; Truong, N. P.; Pei, Z.; Coote, M. L.; Anastasaki, A. Reversing RAFT Polymerization: Near-Quantitative Monomer Generation Via a Catalyst-Free Depolymerization Approach. *J. Am. Chem. Soc.* **2022**, *144*, 4678−4684.
(15) Wang, H. S.; Truong, N. P.; Jones, G. R.; Anastasaki, A. Investigating the Effect of End-Group, Molecular Weight, and Solvents on the Catalyst-Free Depolymerization of RAFT Polymers: Possibility to Reverse the Polymerization of Heat-Sensitive Polymers. *ACS Macro Lett.* **2022**, *11*, 1212−1216.
(16) Häfliger, F.; Truong, N. P.; Wang, H. S.; Anastasaki, A. Fate of the RAFT End-Group in the Thermal Depolymerization of Polymethacrylates. *ACS Macro Lett.* **2023**, *12*, 1207−1212.
(17) Wang, H. S.; Parkatzidis, K.; Junkers, T.; Truong, N. P.; Anastasaki, A. Controlled radical depolymerization: Structural differentiation and molecular weight control. *Chem.* **2024**, *10*, 388−401.
(18) De Alwis Watuthanthrige, N.; Whitfield, R.; Harrisson, S.; Truong, N. P.; Anastasaki, A. Thermal Solution Depolymerization of RAFT Telechelic Polymers. *ACS Macro Lett.* **2024**, *13*, 806−811.
(19) Jeffries, C. M.; Ilavsky, J.; Martel, A.; Hinrichs, S.; Meyer, A.; Pedersen, J. S.; Sokolova, A. V.; Svergun, D. I. Small-angle X-ray and neutron scattering. *Nat. Rev. Methods Primers* **2021**, *1*, 70.
(20) Narayanan, T. Recent advances in synchrotron scattering methods for probing the structure and dynamics of colloids. *Adv. Colloid Interface Sci.* **2024**, *325*, No. 103114.
(21) Roe, R.-J. *Methods of X-ray and Neutron Scattering in Polymer Science*; Oxford University Press, 2000.
(22) Takahashi, R.; Narayanan, T.; Sato, T. Growth Kinetics of Polyelectrolyte Complexes Formed from Oppositely-Charged Homopolymers Studied by Time-Resolved Ultra-Small-Angle X-ray Scattering. *J. Phys. Chem. Lett.* **2017**, *8*, 737−741.
(23) Yamanaka, R.; Sugawara-Narutaki, A.; Takahashi, R. *In Situ* Monitoring of Polymerization-Induced Self-Assembly and Gelation During the Synthesis of Triblock Copolymers *via* Time-Resolved Small-Angle X-ray Scattering and Rheology. *Macromolecules* **2023**, *56*, 4354−4361.
(24) Xu, J.; He, J.; Fan, D.; Tang, W.; Yang, Y. Thermal Decomposition of Dithioesters and Its Effect on RAFT Polymerization. *Macromolecules* **2006**, *39*, 3753−3759.
(25) Chong, B.; Moad, G.; Rizzardo, E.; Skidmore, M.; Thang, S. H. Thermolysis of RAFT-Synthesized Poly(Methyl Methacrylate). *Aust. J. Chem.* **2006**, *59*, 755−762.
(26) Berry, G. C. Thermodynamic and conformational properties of polystyrene. I. Light-scattering studies on dilute solutions of linear polystyrenes. *J. Chem. Phys.* **1966**, *44*, 4550−4564.
(27) Takahashi, R.; Narayanan, T.; Yusa, S.; Sato, T. Kinetics of Morphological Transition between Cylindrical and Spherical Micelles in a Mixture of Anionic−Neutral and Cationic−Neutral Block Copolymers Studied by Time-Resolved SAXS and USAXS. *Macromolecules* **2018**, *51*, 3654−3662.
(28) Takahashi, R.; Qiu, X.-P.; Xue, N.; Sato, T.; Terao, K.; Winnik, F. M. Self-Association of the Thermosensitive Block Copolymer Poly(2-isopropyl-2-oxazoline)-*b*-poly(*N*-isopropylacrylamide) in Water−Methanol Mixtures. *Macromolecules* **2014**, *47*, 6900−6910.
(29) Wei, Y.; Hore, M. J. Characterizing polymer structure with small-angle neutron scattering: A Tutorial. *J. Appl. Phys.* **2021**, *129*, No. 171101.

https://doi.org/10.1021/acspolymersau.4c00095
ACS Polym. Au 2025, 5, 129−133